Progress In Electromagnetics Research Letters, Vol. 98, 155–163, 2021

Compact Four-Band Cactus-Shaped Antenna for 5G and WLAN Applications

Juan Zhang[1, 2], Xiaoming Liu[1, 2, 3, *], Chen Wang[1, 2], Lu Gan[1, 2], Ye Wang[1, 2], and Lijun Sun[3]

Abstract—A low-profile coplanar waveguide fed four-band compact antenna for 5G and WLAN applications is presented in this letter. Multiple bands are generated using a cactus-shaped patch, which consists of several inverted L-shaped slots and branches. The proposed antenna provides 150 MHz (2.10 GHz–2.25 GHz), 400 MHz (3.25 GHz–3.65 GHz), 1022 MHz (4.42 GHz–5.44 GHz), 1400 MHz (5.60 GHz–7.00 GHz) bandwidths of 10 dB return loss, corresponding to the target N1/N78/N79 5G bands and 5.8 GHz WLAN band, respectively. Moreover, the proposed antenna has a low profile of 21 mm × 29 mm × 1.6 mm, while maintaining tolerable gain in these operation bands. In addition, monopole-like radiation patterns are obtained, which is suitable for wireless communication. In order to verify this design, a prototype has been fabricated and measured. The measured results show satisfactory agreement with the simulated ones.

1. INTRODUCTION

With the continued development of communication technology, low-profile multi-band antennas of easy fabrication are required to cover various applications, such as 5G and WLAN. In order to constantly improve the performance of multi-band antennas, much progress has been made [1–18]. Various structures based on patch antenna are reported in [1–7] due to easy integration of antenna to the printed circuit board (PCB). For instance, in [2], multiple resonant modes are provided through F-shaped slots, and circular patches are added on the bottom layer to improve impedance matching so as to increase bandwidth. Furthermore, different types of low-profile multi-band antennas have been investigated for WLAN [8–12]. In [8], a radiating slot is a kind of asymmetric T gap, which can be easily tuned for dual-frequency operation by adjusting the length of the gap. Specifically, multi-band antennas are investigated in [10–12] to meet the needs of laptop computers. Also, multi-band compact multiple-input multiple-output (MIMO) antennas are proposed for 5G in [13–18]. For example, in [15, 16], these antennas adopt multi-curved structures to the radiation patch for overall miniaturization. In the previous antenna research, cactus shape is also often applied. Although all the reported antennas in [1–18] create multiband performance, in comparison, the proposed antenna covers more bands and has a very high area usage efficiency for each band compared to other antennas as shown in Table 1. Particularly, the radiation patterns are monopole like with satisfactory gain. In [19–22], cactus shape radiation structures are used to obtain ultra-wideband or multiband resonance. In [19, 20], wideband has been realized; however, the realized gain is not reported. In [21, 22], tri-band operation is realized, and it is very interesting to find that the realized gain in [22] is less than 0 dB. In addition, the sizes in [19–22] are much larger than the proposed work in this paper.

Received 29 May 2021, Accepted 6 July 2021, Scheduled 12 July 2021

* Corresponding author: Xiaoming Liu (xiaoming.liu@ahnu.edu.cn).

[1] School of Physics and Electronic Information, Anhui Normal University, Wuhu 241002, Anhui, China. [2] Anhui Provincial Engineering Laboratory on Information Fusion and Control of Intelligent Robot, Wuhu 241002, Anhui, China. [3] Wuhu CEPREI Information Industry Technology Research Institute, Wuhu 241002, Anhui, China.

Table 1. Performance comparison of the proposed antenna with reported antennas in the literature.

Ref	Operating bands (GHz)	Size (mm^3)	Peak gain (dB)
[1]	2.3–4, 5–6.6	$40 \times 45 \times 1$	3.2
[2]	2.0–2.76, 3.04–4.0, 5.2–6.0	$19 \times 25 \times 1.6$	3.1
[3]	2.39–2.51, 3.38–3.72, 4.79–6.24	$21 \times 29 \times 1.6$	3.74
[4]	2.29–3.8	$14.8 \times 29.6 \times 1.5$	2.1
[5]	2.35–2.53, 3.34–3.85, 5.05–6.28	$13 \times 27.5 \times 1.6$	2.36
[6]	2.40–2.51, 3.35–3.94, 5.02–6.63	$18 \times 19 \times 1$	2.6
[7]	2.25–2.85, 3.4–4.15, 4.45–8	$15 \times 15 \times 1.6$	3.8
[8]	2.4–2.5, 5.725–5.825	$15 \times 40 \times 0.8$	4.2
[9]	2.38–2.52, 4.92–6.90	$93 \times 135 \times 1.5$	1
[10]	2.4–2.5, 4.6–6.0	$2 \times 40 \times 2$	7.9
[11]	2.4–2.5, 5.1–5.85	$5 \times 20 \times 2.2$	5.6
[12]	2.4–2.5, 5.15–5.85	$5 \times 42 \times 0.8$	4.8
[13]	3.3–3.6, 4.8–5.0	$70 \times 150 \times 0.8$	4.3
[14]	0.824–0.96, 1.71–2.69, 3.4–3.6	$70 \times 140 \times 0.8$	3.7
[15]	1.95–2.5, 3.15–3.85, 4.95–6.6	$40 \times 40 \times 1.6$	4.15
[16]	2.24–2.45, 3.3–4, 5.6–5.75	$48 \times 49 \times 0.8$	–
[17]	2.37–2.64, 3.39–3.58, 4.86–6.98	$25 \times 45 \times 1.57$	–
[18]	3.42–3.6, 4.7–5.1	$44 \times 58 \times 1.2$	4.8
[19]	2.9–12	$28 \times 32 \times 0.225$	–
[20]	0.7–5.6	$150.5 \times 180.97 \times 1.6$	–
[21]	2.32–2.51, 2.72–3.02, 3.39–4.43	$37 \times 71.6 \times 1.524$	–
[22]	2.13–2.48, 3.51–3.88, 5.56–6.70	$45 \times 80 \times 1.5$	−13.96
This work	2.10–2.25, 3.24–3.65, 4.42–5.44, 5.60–7.00	$21 \times 29 \times 1.6$	4.2

In this letter, a low-profile coplanar waveguide fed four-band compact antenna for 5G and WLAN applications is presented. The cactus-shaped patch with inverted L-shaped slots and L-shaped branches is used as a radiator to create four operation bands, covering the 5G bands of N1/N78/N79 (2.11 GHz–2.17 GHz, 3.3 GHz–3.8 GHz, 4.4 GHz–5.0 GHz) and the 5.8 GHz WLAN band (5.725 GHz–5.825 GHz). Such a structure is easy of fabrication and integration with PCB circuits. In addition, the radiation patterns are monopole like with good peak gains in these bands. These properties are preferred in wireless communication.

2. ANTENNA DESIGN

The structure of the proposed microstrip antenna is depicted in Fig. 1. It is shown that the radiator and ground plane are printed on a 1.6 mm thick FR4 dielectric substrate (relative permittivity is 4.4, and loss tangent is 0.02). The geometry of the substrate is a rectangular solid with the size of $21 \times 29 \times 1.6\,mm^3$. The proposed microstrip antenna is fed by coplanar waveguide. The impedance of the SMA connector in our work is 50 Ω, so we have designed the feeding line to be 50 Ω as well. To obtain 50 Ω impedance matching, the calculated width W_f for the feed line is 3.5 mm, and the gap is 0.5 mm. The cactus-shaped patch acts as the radiator of the antenna, which is composed of two inverted L-shaped slots and L-shaped branches. All parameters of the antenna are given in Table 2. The simulation and optimization are performed by using the commercial software ANSYS HFSS 15.

The design evolution is presented in Fig. 2. The antennas of each step are marked as 1 to 4. For antenna 1, three stubs are used, and three operation bands (2.30 GHz–2.39 GHz, 3.20 GHz–3.68 GHz,

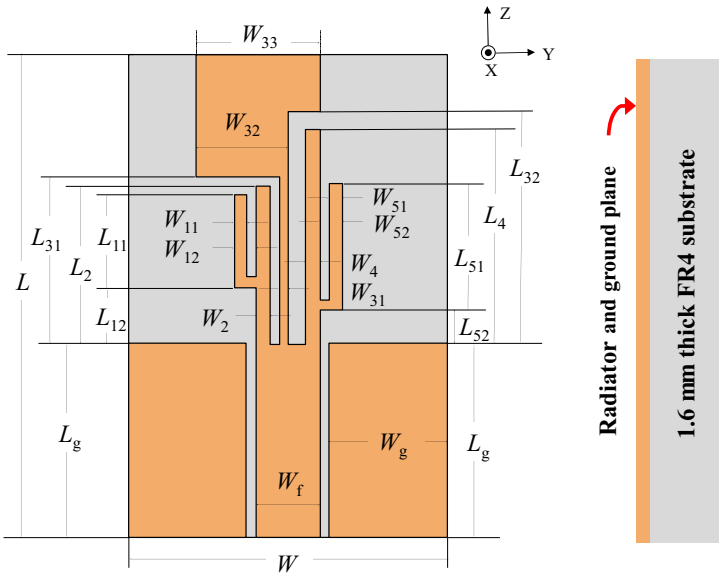

Figure 1. Configuration of the proposed antenna.

Table 2. Parameters of the proposed antenna.

Parameters	Unit (mm)	Parameters	Unit (mm)
L	29	W_g	8.25
L_g	12	W_f	3.5
L_{11}	5.4	W_{11}	0.6
L_{12}	3	W_{12}	1.2
L_2	9	W_2	0.8
L_{31}	9.5	W_{31}	0.3
L_{32}	14.4	W_{32}	5.9
L_4	13.4	W_{33}	7.8
L_{51}	7.8	W_4	0.9
L_{52}	2	W_{51}	0.6
W	21	W_{52}	1

4.78 GHz–6.43 GHz) are created. The middle stub is loaded at the end with a patch to resonate at low frequency. For antenna 2, an L-shaped branch is added to create the fourth band (4.85 GHz–5.18 GHz). This L-shaped branch is added near the feeding line, while a certain distance is maintained to the ground plane to avoid strong coupling to the ground. However, it is clearly seen that the third band has insufficient bandwidth. To solve this problem, another L-shaped branch is added to the left side of Antenna 2. It is seen that the fourth band shows satisfactory bandwidth. The third band also shows good bandwidth. The last issue is related to the N1 5G band, which is determined by the middle stub. To tune the mode to lower frequency, one straightforward way is to prolong the stub, which will inevitably increase the size. For this reason, we further increase the width of the patch to increase the path length of the current. By doing so, the first mode shifts to the N1 band. Meanwhile, other modes do not see obvious change. The bandwidths of each band also meet the requirements.

To further understand the operating principle, the simulated surface current distributions are plotted in Fig. 3 at frequencies of 2.15 GHz, 3.5 GHz, 4.8 GHz, and 5.8 GHz, corresponding to the central frequencies of each band. From Fig. 3(a), one can find that the strong surface current concentrates on the

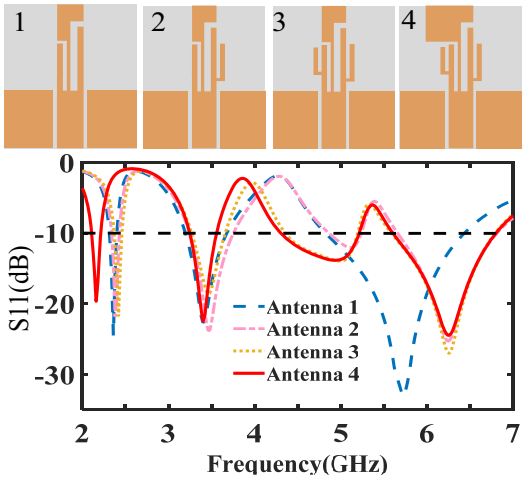

Figure 2. The evolution of the proposed antenna.

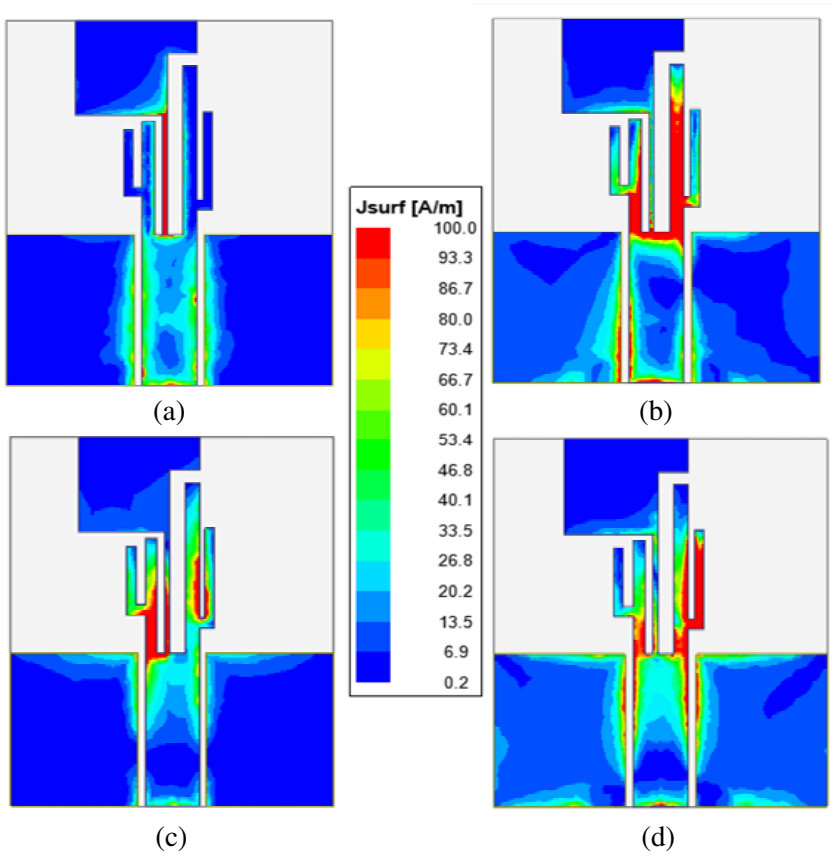

Figure 3. Simulated surface current distributions of the proposed antenna at (a) 2.15 GHz, (b) 3.5 GHz, (c) 4.8 GHz, (d) 5.8 GHz.

central radiation line. Then, the current distributes to the end patch. Therefore, it can be understood that the 2.11 GHz–2.17 GHz N1 5G resonance occurs due to the middle branch. Actually, one could roughly estimate the resonant frequency by using the equation of $f_0 = c/(\lambda_g\sqrt{\varepsilon_{eff}})$, where ε_{eff} is the effective permittivity, and $\lambda_g \approx 4(L - L_g + W_{33})$. The coefficient 4 is because this antenna is a monopole antenna. The calculated frequency is 2.05 GHz, which is very close to the simulated results. For the

3.5 GHz band, the current goes to the second branch on the right side, and part of the current is also seen on the second branch on the left side, as shown in Fig. 3(b). In this connection, one could use $\lambda_g \approx 4(L_4 + W_f/2)$, leading to 3.36 GHz, in good agreement with the simulated value. The reason for involving W_f is that the current has crossed the feed line. The third resonant mode of the antenna arises from the two branches on the left side of the antenna and the central branch, as see in Fig. 3(c). By using two branches, the required bandwidth of the third band can be obtained. The frequency in this case can be predicted using $\lambda_g \approx 4(L_2 + W_f/2)$, giving 4.76 GHz, also within reasonable error. From Fig. 3(d), one can find that the strongest surface current concentrates on the first branch on the right side. This is in line with the design procedure shown in Fig. 2. The frequency prediction can be done by using $\lambda_g \approx 4(L_{51} + W_{51})$, which gives 5.88 GHz, showing a very good agreement with simulation. The calculations indicate that this design method can be easily employed for the operation frequency prediction, which will significantly reduce the optimization time. This observation is obviously supported by the simulated S_{11} in Fig. 2.

Parametric study on several key parameters is plotted in Fig. 4. In Fig. 4(a), it is shown that the width of the central patch (W_{33}) of the radiator is critical to the first resonance. This is because by tuning W_{33}, the first resonance can be changed, while other bands are quite stable, which is in line with the described principle in Fig. 2. In other words, parameter W_{33} influences the equivalent length of the middle branch and consequently affects the resonate frequency. The second band is determined by the length of L_4, as can be seen in Fig. 4(b). The frequency is inversely proportional to the value of L_4. It is also found that with the increase of L_4, S_{11} decreases slightly. However, the bandwidth does see significant variation. Similarly, the parameters of L_2 and L_{51} determine the third and fourth bands.

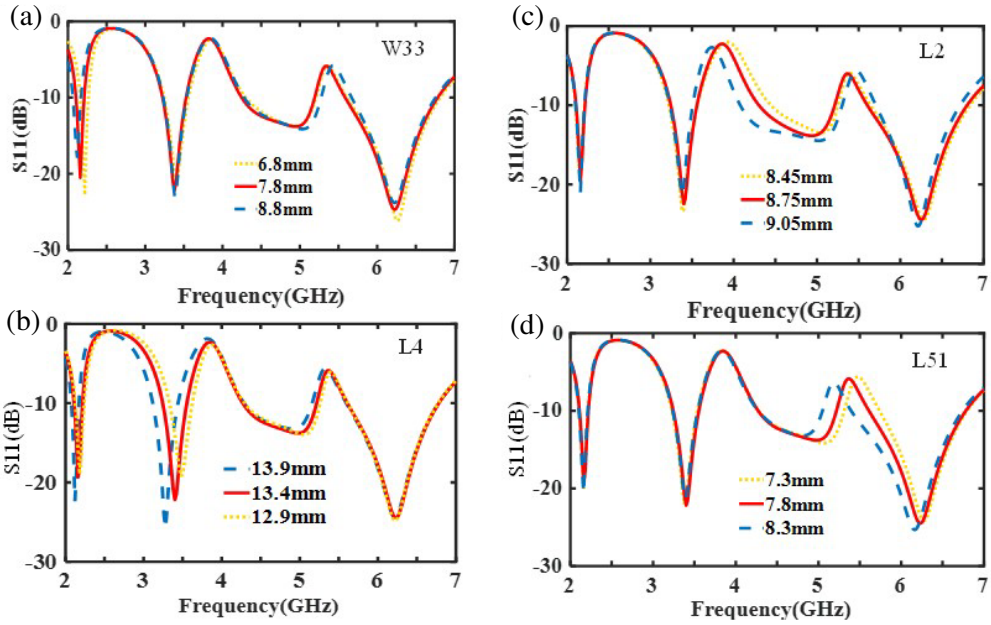

Figure 4. Simulated S_{11} against frequency for the proposed antenna with various units (a) W_{33}, (b) L_4, (c) L_2, (d) L_{51}.

3. MEASUREMENT AND DISCUSSION

The fabricated prototype is shown in Fig. 5 in comparison with a metric ruler. It is clearly seen that this design shows a very compact size. The comparison between measured reflection coefficients S_{11} and simulated ones is plotted in Fig. 6. It is shown that the agreement is good. There is a frequency deviation for band 4. It is likely due to fabrication error, or that the soldering part is more influential to higher frequency. In addition, it shows that the 10 dB impedance bandwidths for the

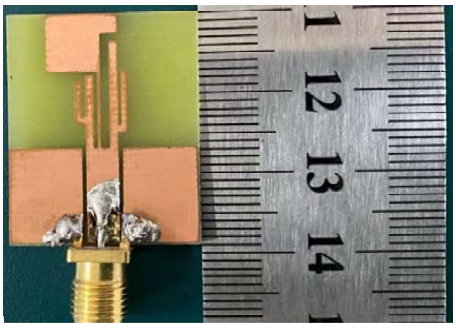

Figure 5. A photography of the fabricated antenna in comparison with a ruler.

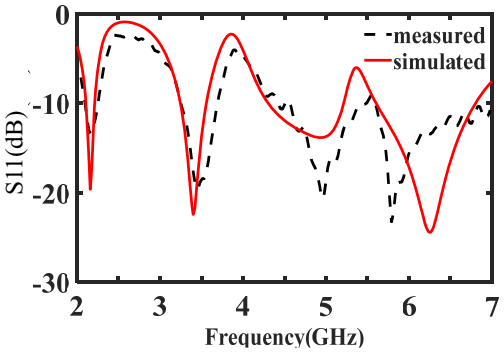

Figure 6. Simulated and measured return losses of the proposed antenna.

four bands are 150 MHz (2.10 GHz–2.25 GHz), 400 MHz (3.25 GHz–3.65 GHz), 1022 MHz (4.42 GHz–5.44 GHz), 1400 MHz (5.60 GHz–7.00 GHz), respectively.

Radiation characteristics, including radiation patterns and peak gains of the antenna have been measured in an anechoic chamber. The measurement was conducted in comparison with a standard horn antenna. The normalized radiation patterns of E-plane and H-plane at 2.15 GHz, 3.5 GHz, 4.8 GHz, and 5.8 GHz are plotted in Fig. 7. Overall, the agreement between measurement and simulation is pretty good. The monopole-like pattern is well recognized. For the last two bands, the patterns in the E-plane are slight distorted, which can be explained by the current distribution in Fig. 3(c) and Fig. 3(d). The cross polarization in the E-plane shows very good omnidirectional form. In the H-plane,

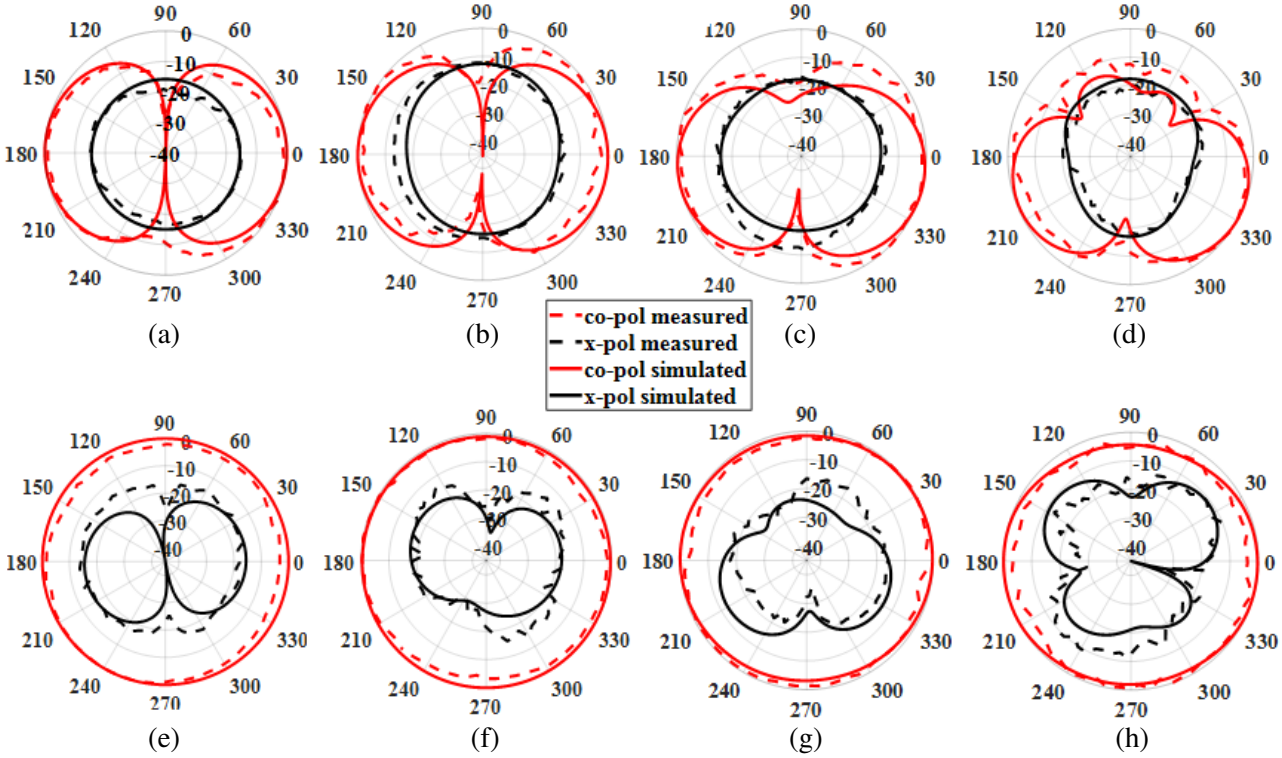

Figure 7. Measured and simulated radiation patterns of the fabricated antenna. (a) 2.15 GHz E-plane, (b) 3.5 GHz E-plane, (c) 4.8 GHz E-plane, (d) 5.8 GHz E-plane, (e) 2.15 GHz H-plane, (f) 3.5 GHz H-plane, (g) 4.8 GHz H-plane, (h) 5.8 GHz H-plane.

the omnidirectional shape can be well seen. Furthermore, it is easy to see that the beam efficiency of the four frequency points of the antenna is very high, and the small side lobe appears only at the highest frequency point. Such properties are preferred for mobile and WLAN communications.

The peak gain over the frequency range of 2 GHz–7 GHz is plotted in Fig. 8. It is demonstrated that the agreement between the measurement and simulation is satisfactory. The feasibility of the proposed antenna is hence verified.

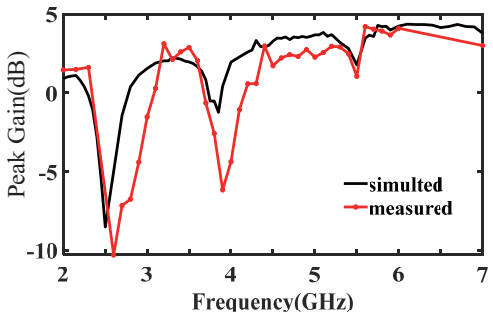

Figure 8. Gain peak of the proposed antenna.

A four-band compact microstrip antenna with coplanar waveguide fed for 5G and WLAN is presented. Multiple bands are generated by using a cactus-shaped patch, which consists of inverted L-shaped slots and L-shaped branches. The proposed antenna can provide impedance bandwidths of 150 MHz (2.10 GHz–2.25 GHz), 400 MHz (3.25 GHz–3.65 GHz), 1022 MHz (4.42 GHz–5.44 GHz), 1400 MHz (5.60 GHz–7.00 GHz) with 10 dB return loss, among which three passbands are in 5G bands, and the remaining one covers 5.8 GHz WLAN band. The realized gains in each band are satisfactory. Monopole-like radiation patterns are obtained for wireless communication.

ACKNOWLEDGMENT

This work is supported by the National Natural Science Foundation of China under the contract number of 61871003 and the open project of the state key laboratory of complex electromagnetic environment effects on electronics and information system under grant number CEMEE2021Z0201B, the Open-ended Foundation of National Radar Signal Processing Laboratory under Grant of 61424100105.

REFERENCES

1. Huang, H., Y. Liu, S. Zhang, and S. Gong, "Multiband metamaterial-loaded monopole antenna for WLAN/WiMAX applications," *IEEE Antennas and Wireless Propagation Letters*, Vol. 14, 662–665, Feb. 2015.
2. Gautam, K., L. Kumar, B. K. Kanaujia, and K. Rambabu, "Design of compact F-shaped slot triple-band antenna for WLAN/WiMAX applications," *IEEE Transactions on Antennas and Propagation*, Vol. 64, No. 3, 1101–1105, 2016.
3. Chen, H., X. Yang, Y. Z. Yin, S. T. Fan, and J. J. Wu, "Triband planar monopole antenna with compact radiator for WLAN/WiMAX applications," *IEEE Antennas and Wireless Propagation Letters*, Vol. 12, 1440–1443, 2013, doi: 10.1109/LAWP.2013.2287312.
4. Zhou, C., G. Wang, J. Liang, Y. Wang, and B. Zong, "Broadband antenna employing simplified MTLs for WLAN/WiMAX applications," *IEEE Antennas and Wireless Propagation Letters*, Vol. 14, 595–598, Apr. 2014.
5. Li, X., X. Shi, W. Hu, P. Fei, and J. Yu, "Compact triband ACS-fed monopole antenna employing open-ended slots for wireless communication," *IEEE Antennas and Wireless Propagation Letters*, Vol. 12, 388–391, 2013, doi: 10.1109/LAWP.2013.2252414.

6. Hu, W., Y. Yin, X. Yang, and P. Fei, "Compact multiresonator-loaded planar antenna for multiband operation," *IEEE Transactions on Antennas and Propagation*, Vol. 61, No. 5, 2838–2841, May 2013, doi: 10.1109/TAP.2013.2242819.
7. Moosazadeh, M. and S. Kharkovsky, "Compact and small planar monopole antenna with symmetrical L- and U-shaped slots for WLAN/WiMAX applications," *IEEE Antennas and Wireless Propagation Letters*, Vol. 13, 388–391, 2014, doi: 10.1109/LAWP.2014.2306962.
8. Wong, K., H. Chang, C. Wang, and S. Wang, "Very-low-profile grounded coplanar waveguide-fed dual-band WLAN slot antenna for on-body antenna application," *IEEE Antennas and Wireless Propagation Letters*, Vol. 19, No. 1, 213–217, Jan. 2020, doi: 10.1109/LAWP.2019.2958961.
9. Nie, M., X. Yang, G. Tan, and B. Han, "A compact 2.45-GHz broadband rectenna using grounded coplanar waveguide," *IEEE Antennas and Wireless Propagation Letters*, Vol. 14, 986–989, Dec. 2015, doi: 10.1109/LAWP.2015.2388789.
10. Lee, C., S. Su, S. Chen, and C. Fu, "Low-cost, direct-fed slot antenna built in metal cover of notebook computer for 2.4-/5.2-/5.8-GHz WLAN operation," *IEEE Transactions on Antennas and Propagation*, Vol. 65, No. 5, 2677–2682, May 2017, doi: 10.1109/TAP.2017.2679070.
11. Su, S., C. Lee, and S. Chen, "Compact, printed, tri-band loop antenna with capacitively-driven feed and end-loaded inductor for notebook computer applications," *IEEE Access*, Vol. 6, 6692–6699, 2018, doi: 10.1109/ACCESS.2018.2794606.
12. Su, S., C. Lee, and S. Chen, "Very-low-profile, triband, two-antenna system for WLAN notebook computers," *IEEE Antennas and Wireless Propagation Letters*, Vol. 17, No. 9, 1626–1629, Sept. 2018, doi: 10.1109/LAWP.2018.2858849.
13. Hu, W., et al., "Dual-band ten-element MIMO array based on dual-mode IFAs for 5G terminal applications," *IEEE Access*, Vol. 7, 178476–178485, 2019, doi: 10.1109/ACCESS.2019.2958745.
14. Ban, Y., C. Li, C. Sim, G. Wu, and K. Wong, "4G/5G multiple antennas for future multi-mode smartphone applications," *IEEE Access*, Vol. 4, 2981–2988, 2016, doi: 10.1109/ACCESS.2016.2582786.
15. Ramachandran, A., S. Mathew, V. Rajan, and V. Kesavath, "A compact triband quad-element MIMO antenna using SRR ring for high isolation," *IEEE Antennas and Wireless Propagation Letters*, Vol. 16, 1409–1412, 2017, doi: 10.1109/LAWP.2016.2640305.
16. Liu, R., X. An, H. Zheng, M. Wang, Z. Gao, and E. Li, "Neutralization line decoupling tri-band multiple-input multiple-output antenna design," *IEEE Access*, Vol. 8, 27018–27026, 2020, doi: 10.1109/ACCESS.2020.2971038.
17. Nandi, S. and A. Mohan, "CRLH unit cell loaded triband compact MIMO antenna for WLAN/WiMAX applications," *IEEE Antennas and Wireless Propagation Letters*, Vol. 16, 1816–1819, 2017, doi: 10.1109/LAWP.2017.2681178.
18. Tan, X., W. Wang, Y. Wu, Y. Liu, and A. A. Kishk, "Enhancing isolation in dual-band meander-line multiple antenna by employing split EBG structure," *IEEE Transactions on Antennas and Propagation*, Vol. 67, No. 4, 2769–2774, Apr. 2019, doi: 10.1109/TAP.2019.28974.
19. Nikolaou, S., G. E. Ponchak, M. M. Tentzeris, and J. Papapolymerou, "Compact cactus-shaped ultra wide-band (UWB) monopole on organic substrate," *2007 IEEE Antennas and Propagation Society International Symposium*, 4637–4640, 2007, doi: 10.1109/APS.2007.4396577.
20. Eveleigh, E., A. S. Beaverstone, and N. K. Nikolova, "Printed Cactus monopole antenna with enhanced impedance bandwidth," *2019 IEEE International Symposium on Antennas and Propagation and USNC-URSI Radio Science Meeting*, 1085–1086, 2019, doi: 10.1109/APUSNCURSINRSM.2019.8888729.
21. Zachou, V., C. G. Christodoulou, M. T. Chryssomallis, and D. Anagnostou, "Reconfigurable printed cactus antenna," *2006 IEEE Antennas and Propagation Society International Symposium*, 201–204, 2006, doi: 10.1109/APS.2006.1710489.
22. Saephan, C., H. Khaleel, B. Valdovinos, A. Isaac, and A. Bihnam, "Tri-band cactus shaped printed monopole," *2014 IEEE Antennas and Propagation Society International Symposium (APSURSI)*, 1704–1705, 2014, doi: 10.1109/APS.2014.6905178.

23. Morabito, A. F., A. R. Laganà, and T. Isernia, "Optimizing power transmission in given target areas in the presence of protection requirements," *IEEE Antennas and Wireless Propagation Letters*, Vol. 14, 44–47, 2015, doi: 10.1109/LAWP.2014.2354514.